Available online at www.sciencedirect.com
ScienceDirect
Journal of Sound and Vibration 303 (2007) 659–674
JOURNAL OF SOUND AND VIBRATION
www.elsevier.com/locate/jsvi

On measures of nonlinearity effects for uncertain dynamical systems—Application to a vibro-impact system

Rubens Sampaio[a,*], Christian Soize[b]

[a]*Pontifícia Universidade Católica do Rio de Janeiro, Departamento de Engenharia Mecânica, Rua Marquês de São Vicente 225, Gávea, 22453-900, Rio de Janeiro, RJ, Brazil*

[b]*Universite de Marne la Vallee, Laboratoire de Mecanique 5 Bd Descartes, Champs sur Marne, 77454 Marne la Vallee, France*

Received 6 June 2005; received in revised form 15 December 2006; accepted 19 January 2007
Available online 28 March 2007

Abstract

The transient dynamics of a linear dynamical system with elastic barriers is studied. The system is excited by a deterministic transient force whose Fourier transform is limited to a narrow frequency band. As the system responds it may impact the elastic barrier, therefore, the system behavior is nonlinear. In order to measure the degree of nonlinearity of the system, one looks for the mechanical energy transferred outside the frequency band of excitation as a function of the parameter η defined by ε/a, in which ε is the size of the barrier gap and a is the amplitude of the excitation force. The mechanical energy transferred outside the frequency band of excitation can potentially be a source of excitation for other subsystems. Consequently, quantification of this energy transfer is an important step in developing an understanding of the nonlinear dynamical system behavior. In addition, it is well known that this type of nonlinear dynamical system is very sensitive to uncertainties. For this reason the system is considered to be deterministic and also stochastic in order to take into account random uncertainties. The proposed analysis is applied to a Timoshenko beam having its motion constrained by a symmetric elastic barrier at its free end. The confidence region of the random mechanical energy transferred outside the excitation band is shown as a function of η for several levels of model and data uncertainties. From this, the robustness of the predictions can be analyzed with respect to model and data uncertainties.

1. Introduction

The nonlinear dynamics of linear dynamical systems with barriers inducing impacts has received considerable attention in the last two decades. Although there are some engineering systems where impacts are part of the project, most of the time this phenomenon is related to wear, fatigue and noise as, for example, in the case of gear boxes. The interest in vibro-impact systems arises due to their intrinsic nonlinear characteristic which prevents their study through more traditional methods such as modal analysis. Actually, systems of this kind have extremely complex dynamic behavior, sometimes even chaotic. Therefore, they are normally studied with bifurcation diagrams and Poincaré maps. However, most of the vibro-impact systems investigated so far consist of simple ones with a single degree of freedom. It is expected that the flexibility of a structure will play

*Corresponding author. Tel.: +55 21 3114 1172; fax: +55 21 3314 1165.
E-mail addresses: rsampaio@mec.puc-rio.br (R. Sampaio), soize@univ-mlv.fr (C. Soize).

0022-460X/$ - see front matter © 2007 Elsevier Ltd. All rights reserved.
doi:10.1016/j.jsv.2007.01.033

an important role in its impact response, especially through the excitations of many of its degrees of freedom. Also one expects some exchange of energy among modes due to impacts. A lot of works have been published concerning one single degree of freedom and multi-degrees of freedom deterministic systems excited by deterministic harmonic signals or by narrow- or wide-band stochastic processes (see for instance Ref. [1]). Some works were also published on the identification of restoring force nonlinearities from the system response to white noise excitation (see for instance [2] for single degree of freedom systems). A review of such works can be found in the recent paper by Dimentberg and Iourtchenko [3]. It should be noted that deterministic continuous systems with impacts have received less attention, probably because of the difficulties of analyzing these types of nonlinear dynamical problems using analytical or numerical methods. However, some recent representative works of this type can be found in Refs. [4–8].

Some of the features of this work are:

- The linear system is not a single-, nor a multiple-degree-of-freedom system, it is a continuous system. Nevertheless, in order to simplify the presentation and also to show that the methodology applies to a general dynamical system, we start with a discretization of the continuous system by using finite element methods.
- The excitation is not a narrow-nor a broad-band stochastic process (including white noise), nor is it a deterministic harmonic signal. In this paper the excitation will be modelled as a deterministic narrow-band signal. This choice is important because it gives some robustness to the excitation. The band is centered around one of the natural frequencies of the linear system (without impact) and the width of the band is chosen in order to allow for modifications of the system to be taken into account (nonlinearities and uncertainties).
- It deals with deterministic and also stochastic modelling of the continuous system. The stochastic aspects being induced by the uncertainties in the data and in the model (the matrices that represent the linear continuous system are random).
- Measures of nonlinearities are proposed. In order to analyze the degree of nonlinearity of the system, one looks for the mechanical energy transferred outside the frequency band of excitation as a function of the parameter η, defined by ε/a, where ε is the size of the barrier gap and a is the amplitude of the excitation force. When ε is zero or infinity, there are no impacts. When it is between this two bounds the continuous system-barrier behaves nonlinearly for a sufficiently high amplitude a. It turns out that the nonlinearity depends on η. The the amount of energy that is transferred outside the band of excitation is measured to evaluate the possiblity of dangerous consequences like exciting sensitive subsystems whose lowest eigenfrequency is outside the band of excitation.
- Stochastic systems are considered in order to evaluate the robustness of the numerical prediction of the energy transferred with respect to data and model uncertainties.

This paper is divided into four parts. Section 2 is devoted to the modelling and analysis of the deterministic nonlinear dynamical system. In Section 3 the stochastic modelling of the system in order to take into account data and model uncertainties is presented. Section 4 deals with numerical applications; the example used is a Timoshenko beam with an elastic barrier. Finally, general analysis and conclusions are presented in Section 5.

2. Modelling and analysis of the deterministic nonlinear dynamical system

In this section the mean model of the dynamical system with excitation; the reduced mean model obtained by using the elastic modes of the linear mean dynamical system; and, finally, the different energies one needs to analyze the energy transferred outside the excitation band are described.

2.1. Finite element model of the mean nonlinear dynamical system

The main theme of the paper is a study of a linear continuous system with elastic barriers that induce nonlinearities through impact. However the methodology presented is general and can be applied to a larger class of problems, as, for example, those related to a linear system interacting with a subsystem that has

nonlinearities, as is the case with an elastic barrier. In the methodology one starts with a finite dimensional system that could be the result of a discretization process. This system, referred to as the *mean model*, is described by the following matrix equation in $\mathbb{R}^m$,

$$[\mathbb{M}]\ddot{\mathbf{y}}(t) + [\mathbb{D}]\dot{\mathbf{y}}(t) + [\mathbb{K}]\mathbf{y}(t) + \mathbf{f}_{\mathrm{NL}}(\mathbf{y}(t), \dot{\mathbf{y}}(t)) = \mathbf{f}(t), \tag{1}$$

where $[\mathbb{M}], [\mathbb{D}], [\mathbb{K}]$ are the mass, damping, and stiffness matrices, that are supposed to be symmetric and positive-definite real matrices, $\mathbf{y}(t)$ is the displacement vector, $\mathbf{f}_{\mathrm{NL}}(\mathbf{y}(t), \dot{\mathbf{y}}(t))$ describes the nonlinear vector forces, and $\mathbf{f}(t)$ is the applied vector load. The nonlinear mapping $(\mathbf{y}, \mathbf{z}) \mapsto \mathbf{f}_{\mathrm{NL}}(\mathbf{y}, \mathbf{z})$ is assumed to be such that $\mathbf{f}_{\mathrm{NL}}(0, 0) = 0$. The vector load $\mathbf{f}(t)$ is written as

$$\mathbf{f}(t) = a g(t) \mathbf{f}_0 \tag{2}$$

in which a is the amplitude and $\mathbf{f}_0$ is a normalized vector describing the position of the applied forces. The impulse $t \mapsto g(t)$ is a square integrable real-valued function on $\mathbb{R}$ whose Fourier transform $\omega \mapsto \widehat{g}(\omega) = \int_{\mathbb{R}} \mathrm{e}^{-\mathrm{i}\omega t} g(t)\, \mathrm{d}t$ has a bounded support $\underline{B}_2 \cup B_2$ with

$$B_2 = [\omega_{\min}, \omega_{\max}], \quad \underline{B}_2 = [-\omega_{\max}, -\omega_{\min}]. \tag{3}$$

The notation B_2 will be explained in Section 2.3. In addition, it is assumed that $\max_{\omega \in B_2} |\widehat{g}(\omega)| = 1$.

2.2. Reduced mean model

Let $\{\phi_1, \ldots, \phi_m\}$ be an algebraic basis of $\mathbb{R}^m$. The reduced mean model of the dynamic system whose mean finite element model is defined by Eq. (1) is obtained by projection of Eq. (1) on the subspace V_n of $\mathbb{R}^m$ spanned by $\{\phi_1, \ldots, \phi_n\}$ with $n \ll m$. Let $[\Phi_n]$ be the $(m \times n)$ real matrix whose columns are the vectors $\{\phi_1, \ldots, \phi_n\}$. The generalized applied force $\mathbf{F}^n(t)$ is an $\mathbb{R}^n$-vector such that $\mathbf{F}^n(t) = [\Phi_n]^{\mathrm{T}} \mathbf{f}(t)$. The generalized mass, damping, and stiffness matrices, $[\underline{M}_n]$, $[\underline{D}_n]$, and $[\underline{K}_n]$, are positive-definite symmetric $(n \times n)$ real matrices such that $[\underline{M}_n] = [\Phi_n]^{\mathrm{T}}[\mathbb{M}][\Phi_n]$, $[\underline{D}_n] = [\Phi_n]^{\mathrm{T}}[\mathbb{D}][\Phi_n]$, and $[\underline{K}_n] = [\Phi_n]^{\mathrm{T}}[\mathbb{K}][\Phi_n]$. Consequently, the reduced mean model of the nonlinear dynamic system, written as the projection $\mathbf{y}^n$ of $\mathbf{y}$ on V_n, can be written as

$$\mathbf{y}^n(t) = [\Phi_n]\mathbf{q}^n(t) \tag{4}$$

in which the vector $\mathbf{q}^n(t) \in \mathbb{R}^n$ of the generalized coordinates verifies the mean nonlinear differential equation,

$$[\underline{M}_n]\ddot{\mathbf{q}}^n(t) + [\underline{D}_n]\dot{\mathbf{q}}^n(t) + [\underline{K}_n]\mathbf{q}^n(t) + \mathbf{F}^n_{NL}(\mathbf{q}^n(t), \dot{\mathbf{q}}^n(t)) = \mathbf{F}^n(t), \tag{5}$$

where, for all $\mathbf{q}$ and $\mathbf{p}$ in $\mathbb{R}^n$,

$$\mathbf{F}^n_{\mathrm{NL}}(\mathbf{q}, \mathbf{p}) = [\Phi_n]^{\mathrm{T}} \mathbf{f}_{\mathrm{NL}}([\Phi_n]\mathbf{q}, [\Phi_n]\mathbf{p}). \tag{6}$$

2.3. Quantification of the transferred energies outside the excitation band

The objective of this section is to quantify the mechanical energy transferred outside the excitation band. It is assumed that Eq. (1) has a unique solution $t \mapsto \mathbf{y}(t)$ such that $\mathbf{y}$ and $\dot{\mathbf{y}}$ are square integrable vector-valued functions on $\mathbb{R}$. An approximation of this solution is computed by using the reduced mean model defined by Eqs. (4)–(6). The positive frequency band $\mathbb{R}^+ = [0, +\infty[$ is then written as

$$\mathbb{R}^+ = [0, +\infty[= B_1 \cup B_2 \cup B_3 \tag{7}$$

in which $B_1 = [0, \omega_{\min}[$ and $B_3 =]\omega_{\max}, +\infty[$. The sets B_1 and B_3 are the bands outside the frequency band of excitation B_2. The total mechanical energy, denoted by $\widetilde{e}$, of the nonlinear dynamical system corresponding to the solution mentioned above is written as

$$\widetilde{e} = \int_{\mathbb{R}} \left(\frac{1}{2} \langle [\mathbb{M}]\dot{\mathbf{y}}(t), \dot{\mathbf{y}}(t) \rangle + \frac{1}{2} \langle [\mathbb{K}]\mathbf{y}(t), \mathbf{y}(t) \rangle \right) \mathrm{d}t. \tag{8}$$

Let $\widehat{\mathbf{y}}(\omega) = \int_{\mathbb{R}} \mathrm{e}^{-\mathrm{i}\omega t}\mathbf{y}(t)\,\mathrm{d}t$ be the Fourier transform of $\mathbf{y}$. Using the Parseval formula, Eq. (8) yields

$$\widetilde{e} = \int_{\mathbb{R}} \underline{h}(\omega)\,\mathrm{d}\omega = 2\int_{\mathbb{R}^+} \underline{h}(\omega)\,\mathrm{d}\omega \tag{9}$$

in which $\underline{h}(\omega)$ is the density of the mechanical energy in the frequency domain which is written as

$$\underline{h}(\omega) = \frac{1}{2\pi}\left\{\frac{1}{2}\langle\omega^2[\mathbb{M}]\widehat{\mathbf{y}}(\omega), \overline{\widehat{\mathbf{y}(\omega)}}\rangle + \frac{1}{2}\langle[\mathbb{K}]\widehat{\mathbf{y}}(\omega), \overline{\widehat{\mathbf{y}(\omega)}}\rangle\right\}. \tag{10}$$

From Eqs. (7) and (9), it can deduced that

$$\widetilde{e} = \widetilde{e}_1 + \widetilde{e}_2 + \widetilde{e}_3 \tag{11}$$

in which

$$\widetilde{e}_j = 2\int_{B_j} \underline{h}(\omega)\,\mathrm{d}\omega, \quad j = 1, 2, 3. \tag{12}$$

The transferred mechanical energy outside the excitation band B_2 is denoted by $\widetilde{e}_{13}$ which is defined by

$$\widetilde{e}_{13} = \widetilde{e}_1 + \widetilde{e}_3. \tag{13}$$

By using the reduced mean model defined by Eqs. (4)–(6), the approximation $\underline{h}^n(\omega)$ of $\underline{h}(\omega)$ defined by Eq. (10) can be written as

$$\underline{h}^n(\omega) = \frac{1}{2\pi}\left\{\frac{1}{2}\langle\omega^2[\underline{M}_n]\widehat{\mathbf{q}}^n(\omega), \overline{\widehat{\mathbf{q}}^n(\omega)}\rangle + \frac{1}{2}\langle[\underline{K}_n]\widehat{\mathbf{q}}^n(\omega), \overline{\widehat{\mathbf{q}}^n(\omega)}\rangle\right\} \tag{14}$$

in which $\widehat{\mathbf{q}}^n(\omega) = \int_{\mathbb{R}} \mathrm{e}^{-\mathrm{i}\omega t}\mathbf{q}^n(t)\,\mathrm{d}t$ is the Fourier transform of $\mathbf{q}^n$. The corresponding energies computed with this approximation are denoted by $\widetilde{e}^n$, $\widetilde{e}^n_1$, $\widetilde{e}^n_2$, $\widetilde{e}^n_3$, $\widetilde{e}^n_{13}$. In order to explore the results in a non-dimensional way one introduces the following parameters:

$$e^n_1 = \frac{\widetilde{e}^n_1}{\widetilde{e}^n}, \quad e^n_2 = \frac{\widetilde{e}^n_2}{\widetilde{e}^n}, \quad e^n_3 = \frac{\widetilde{e}^n_3}{\widetilde{e}^n}, \quad e^n_{13} = \frac{\widetilde{e}^n_{13}}{\widetilde{e}^n}. \tag{15}$$

Consequently, one has,

$$e^n_1 + e^n_2 + e^n_3 = 1, \quad e^n_{13} + e^n_2 = 1. \tag{16}$$

The e^n_{13} represents the percentage of mechanical energy transferred outside the frequency band of the excitation.

3. Modelling and analysis of the nonlinear dynamical system with random uncertainties

The first source of uncertainties in this type of problem is due to the mathematical-mechanical modelling process leading to the boundary value problem. This type of uncertainty is structural, and cannot be represented as, simply, the usual variation of parameters [9,10]. These uncertainties are called *the model uncertainties*. The second source of uncertainties come from parameters such as geometry, material properties, boundary and initial conditions, etc. The uncertainties in these parameters are called *data uncertainties*. It is worthwhile to remark that the errors related to the construction of an approximation of the solution of the boundary value problem, that have to be controlled in order to meet the specifications of the numerical approximation, are not uncertainties.

For the class of systems studied here the sources of uncertainties are in the data related to the nonlinear term and in the data and model associated with the linear part of the system.

3.1. Probabilistic modelling of uncertainties

From this point one constructs a probability model of uncertainties from the mean reduced model defined by Eqs. (4)–(6). All the random variables are defined in a probability space $(\Theta, \mathscr{F}, \mathscr{P})$.

3.1.1. Parametric probabilistic model of data uncertainties for the nonlinear term

Usually, data uncertainties are modelled by using a parametric probabilistic approach consisting of modelling each uncertain parameter by a random variable whose probability distribution has to be constructed using the available information. The nonlinear term $\mathbf{F}^n_{\mathrm{NL}}(\mathbf{q}^n(t), \dot{\mathbf{q}}^n(t))$ in Eq. (5) is rewritten as $\mathbf{F}^n_{\mathrm{NL}}(\mathbf{q}^n(t), \dot{\mathbf{q}}^n(t); \mathbf{s})$ in which $\mathbf{s}$ is an $\mathbb{R}^\nu$-vector of uncertain parameters. The probabilistic modelling of vector $\mathbf{s}$ is as a $\mathbb{R}^\nu$-valued random variable whose probability distribution on $\mathbb{R}^\nu$ is denoted by $P_{\mathbf{S}}(\mathrm{d}\mathbf{s})$. The available information for constructing $P_{\mathbf{S}}(\mathrm{d}\mathbf{s})$ depends on the nature of the parameters constituting the vector $\mathbf{s}$ (for instance, positivity, boundedness of components, etc.). When this information is defined the probability distribution can be constructed by using the maximum entropy principle with the constraints defined by the available information [11–13].

3.1.2. Non-parametric probabilistic model of model and data uncertainties for the linear part

Model uncertainties cannot be taken into account by using the parametric probabilistic approach. A non-parametric probabilistic approach can be used to take into account model uncertainties and data uncertainties [9,10]. The principle of construction for such a non-parametric probabilistic approach to uncertainties, for the linear part of the nonlinear dynamical system whose reduced mean model is defined by Eqs. (4)–(6), consists of replacing the generalized mass, damping, and stiffness matrices in Eq. (5) by the random matrices $[\mathbf{M}_n]$, $[\mathbf{D}_n]$, and $[\mathbf{K}_n]$ whose probability distributions have been constructed by using the maximum entropy principle with an adapted available information. The explicit form of the probability distributions of the random matrices $[\mathbf{M}_n]$, $[\mathbf{D}_n]$, and $[\mathbf{K}_n]$ are given in Refs. [9,10].

3.1.3. Stochastic reduced model

The stochastic transient response of the nonlinear dynamic system, constructed by using a non-parametric probabilistic approach for model and data uncertainties, is the stochastic process $\mathbf{Y}^n(t)$, indexed by $\mathbb{R}$, with values in $\mathbb{R}^m$, such that

$$\mathbf{Y}^n(t) = [\Phi_n]\mathbf{Q}^n(t). \tag{17}$$

The stochastic process $\mathbf{Q}^n$, defined in the probability space $(\Theta, \mathscr{T}, \mathscr{P})$, indexed by $\mathbb{R}$, with values $\mathbb{R}^n$, is such that

$$[\mathbf{M}_n]\ddot{\mathbf{Q}}^n(t) + [\mathbf{D}_n]\dot{\mathbf{Q}}^n(t) + [\mathbf{K}_n]\,\mathbf{Q}^n(t) + \mathbf{F}^n_{\mathrm{NL}}(\mathbf{Q}^n(t), \dot{\mathbf{Q}}^n(t); \mathbf{S}) = \mathbf{F}^n(t) \quad \forall t \in \mathbb{R}. \tag{18}$$

Let $|||\mathbf{Q}^n|||$ be the norm such that

$$|||\mathbf{Q}^n|||^2 = \mathscr{E}\left\{\int_{\mathbb{R}} \|\mathbf{Q}^n(t)\|^2 \,\mathrm{d}t\right\}, \tag{19}$$

where $\mathscr{E}$ is the mathematical expectation and $\|\mathbf{u}\|^2 = u_1^2 + \cdots + u_n^2$ is the square of the Euclidean norm of $\mathbf{u}$ in $\mathbb{R}^n$. It is assumed that the nonlinear term is such that Eq. (18) has a unique second-order mean-square solution such that

$$|||\mathbf{Q}^n||| < +\infty, \quad |||\dot{\mathbf{Q}}^n||| < +\infty. \tag{20}$$

3.2. Probabilistic quantification of the transferred energies outside the excitation band for the uncertain system

The next step is to adapt the methodology described in Section 2.3 so that it can be applied to the reduced stochastic system defined by Eqs. (17) and (18). The random total mechanical energy associated with $\widetilde{e}^n$ is denoted by $\widetilde{E}^n$ and is such that

$$\widetilde{E}^n = \int_{\mathbb{R}} \left(\frac{1}{2}\langle [\mathbb{M}]\dot{\mathbf{Y}}^n(t), \dot{\mathbf{Y}}^n(t)\rangle + \frac{1}{2}\langle [\mathbb{K}]\mathbf{Y}^n(t), \mathbf{Y}^n(t)\rangle \right) \mathrm{d}t. \tag{21}$$

The density of the random mechanical energy in the frequency domain associated with $\underline{h}^n(\omega)$ defined by Eq. (14) is denoted by $H^n(\omega)$ and can be written as

$$H^n(\omega) = \frac{1}{2\pi}\left\{\frac{1}{2}\langle\omega^2[\underline{M}_n]\widehat{\mathbf{Q}}^n(\omega), \overline{\widehat{\mathbf{Q}}^n(\omega)}\rangle + \frac{1}{2}\langle[\underline{K}_n]\widehat{\mathbf{Q}}^n(\omega), \overline{\widehat{\mathbf{Q}}^n(\omega)}\rangle\right\} \tag{22}$$

in which $\widehat{\mathbf{Q}}^n(\omega) = \int_{\mathbb{R}} \mathrm{e}^{-\mathrm{i}\omega t}\mathbf{Q}^n(t)\,\mathrm{d}t$ is the Fourier transform of $\mathbf{Q}^n$.

Let $H^n_{\mathrm{dB}}(\omega)$ be the density of the random mechanical energy in dB normalized with respect to the total mechanical energy $\widetilde{e}_{\mathrm{lin}}$ of the linear mean system, thus

$$H^n_{\mathrm{dB}}(\omega) = \log_{10}(H^n(\omega)/\widetilde{e}_{\mathrm{lin}}). \tag{23}$$

Let $\widetilde{E}^n_1$, $\widetilde{E}^n_2$, $\widetilde{E}^n_3$ and $\widetilde{E}^n_{13}$ be the random energies associated with $\widetilde{e}^n_1$, $\widetilde{e}^n_2$, $\widetilde{e}^n_3$ and $\widetilde{e}^n_{13}$ such that

$$\widetilde{E}^n_j = 2\int_{B_j} H^n(\omega)\,\mathrm{d}\omega, \quad j = 1,2,3, \quad \widetilde{E}^n_{13} = \widetilde{E}^n_1 + \widetilde{E}^n_3. \tag{24}$$

As in Section 2.3, this random energies are normalized:

$$E^n_1 = \frac{\widetilde{E}^n_1}{\widetilde{E}^n}, \quad E^n_2 = \frac{\widetilde{E}^n_2}{\widetilde{E}^n}, \quad E^n_3 = \frac{\widetilde{E}^n_3}{\widetilde{E}^n}, \quad E^n_{13} = \frac{\widetilde{E}^n_{13}}{\widetilde{E}^n}. \tag{25}$$

Consequently, the random energies satisfy:

$$E^n_1 + E^n_2 + E^n_3 = 1, \quad E^n_{13} + E^n_2 = 1. \tag{26}$$

E^n_{13} represents the percentage of the random mechanical energy transferred outside the frequency band of the excitation.

3.3. Stochastic solver and convergence

In this section a stochastic solver is introduced and the stochastic convergence is analyzed. The Monte Carlo numerical simulation and mathematical statistics are used for solving the stochastic equations defined by Eqs. (17) and (18). Let $\mathbf{S}(\theta)$, $[\mathbf{M}_n(\theta)]$, $[\mathbf{D}_n(\theta)]$ and $[\mathbf{K}_n(\theta)]$ be independent realizations of the random variable $\mathbf{S}$ and the random matrices $[\mathbf{M}_n]$, $[\mathbf{D}_n]$ and $[\mathbf{K}_n]$, respectively, for $\theta \in \Theta$.

3.3.1. Construction of realizations of random variable $\mathbf{S}$

Each realization $\mathbf{S}(\theta)$ of random variable $\mathbf{S}$ is usually constructed by using a random generator associated with the probability distribution $P_{\mathbf{S}}(\mathrm{d}\mathbf{s})$. Because the generation is standard details will not be given here.

3.3.2. Construction of realizations of random matrix variables $[\mathbf{M}_n]$, $[\mathbf{D}_n]$, $[\mathbf{K}_n]$

Let $[\mathbf{A}_n]$ be any of the three random matrices above and let $[\underline{\mathbf{A}}_n]$ be its mean value which is a positive-definite matrix. Its Cholesky factorization yields $[\underline{\mathbf{A}}_n] = [\underline{L}_n]^{\mathrm{T}}[\underline{L}_n]$. Each realization $[\mathbf{A}_n(\theta)]$ can be generated by using the following algebraic representation [9,10]:

$$[\mathbf{A}_n] = [\underline{L}_n]^{\mathrm{T}}[\mathbf{G}_n][\underline{L}_n] \tag{27}$$

in which the positive-definite random matrix $[\mathbf{G}_n]$ is written as

$$[\mathbf{G}_n] = [\mathbf{L}_n]^{\mathrm{T}}[\mathbf{L}_n]. \tag{28}$$

In Eq. (28), $[\mathbf{L}_n]$ is an upper triangular random matrix with values in $\mathbb{M}_n(\mathbb{R})$ such that:

(1) The random variables $\{[\mathbf{L}_n]_{jj'}, j \leqslant j'\}$ are independent.
(2) For $j < j'$, the real-valued random variable $[\mathbf{L}_n]_{jj'}$ can be written as $[\mathbf{L}_n]_{jj'} = \sigma_n U_{jj'}$ in which $\sigma_n = \delta(n+1)^{-1/2}$ and where $U_{jj'}$ is a real-valued Gaussian random variable with zero mean and variance equal to 1.
(3) For $j = j'$, the positive-valued random variable $[\mathbf{L}_n]_{jj}$ can be written as $[\mathbf{L}_n]_{jj} = \sigma_n\sqrt{2V_j}$ in which σ_n is defined above and where V_j is a positive-valued gamma random variable whose probability density

function $p_{V_j}(v)$ with respect to $\mathrm{d}v$ is written as

$$p_{V_j}(v) = \mathbf{1}_{\mathbb{R}^+}(v)\frac{1}{\Gamma\left(\dfrac{n+1}{2\delta^2}+\dfrac{1-j}{2}\right)}v^{(n+1/2\delta^2)-(1+j/2)}\mathrm{e}^{-v}, \tag{29}$$

where $\mathbf{1}_{\mathbb{R}^+}(v) = 1$ if $v \in \mathbb{R}^+$ and $= 0$ if not, and where Γ is the usual Gamma function. This algebraic representation includes δ which is a positive parameter allowing control of the dispersion of the random matrix $[\mathbf{A}_n]$. This parameter has to be given for each random matrix and controls the level of uncertainties. In particular, it controls the uncertainties of mass, damping or stiffness of the linear continuous system of the nonlinear dynamical system.

3.3.3. Construction of realizations of the solution of the stochastic reduced system

The realization $\mathbf{Y}^n(t,\theta)$ for $\theta \in \Theta$ of $\mathbf{Y}^n(t)$ defined by Eq. (17) is given by

$$\mathbf{Y}^n(t,\theta) = [\Phi_n]\mathbf{Q}^n(t,\theta) \tag{30}$$

in which the realization $\{\mathbf{Q}^n(t,\theta), t \in \mathbb{R}\}$ of the stochastic process $\{\mathbf{Q}^n(t), t \in \mathbb{R}\}$, is the solution of the following deterministic nonlinear reduced equation:

$$\begin{aligned}&[\mathbf{M}_n(\theta)]\ddot{\mathbf{Q}}^n(t,\theta) + [\mathbf{D}_n(\theta)]\dot{\mathbf{Q}}^n(t,\theta) + [\mathbf{K}_n(\theta)]\mathbf{Q}^n(t,\theta)\\ &\quad + \mathbf{F}^n_{NL}(\mathbf{Q}^n(t,\theta), \dot{\mathbf{Q}}^n(t,\theta); \mathbf{S}(\theta)) = \mathbf{F}^n(t,\theta) \quad \forall t \in \mathbb{R}.\end{aligned} \tag{31}$$

This equation is solved by using an implicit unconditionally stable scheme such as the Newmark algorithm. At each time step, the nonlinear algebraic equation coming from the scheme is solved by iteration.

3.3.4. Stochastic convergence

The mean-square convergence of the second-order stochastic solution of Eq. (18) with respect to dimension n of the stochastic reduced model and to the number n_s of realizations used in the Monte Carlo numerical simulations is controlled by the norm $|||\mathbf{Q}^n|||$ defined by Eq. (19). By using the usual estimation of the mathematical expectation operator $\mathscr{E}$, convergence with respect to n and n_s is studied by constructing the function $(n_s, n) \mapsto \mathrm{conv}(n_s, n)$ defined by

$$\mathrm{conv}(n_s,n) = \left\{\frac{1}{n_s}\sum_{k=1}^{n_s}\int_{\mathbb{R}}\|\mathbf{Q}^n(t,\theta_k)\|^2\,\mathrm{d}t\right\}^{1/2} \tag{32}$$

in which $\mathbf{Q}^n(t,\theta_1),\ldots,\mathbf{Q}^n(t,\theta_{n_s})$ are n_s independent realizations of $\mathbf{Q}^n(t)$.

3.3.5. Statistical estimations of the random energies

It is of interest to construct statistical estimations for the stochastic process $\{H^n(\omega), \omega \in \mathbb{R}\}$ defined by Eq. (22) and for the random variables E^n_1, E^n_2, E^n_3, E^n_{13} defined by Eq. (24), whose realizations are directly deduced from the realizations of $\mathbf{Q}^n$. Let X be the positive-valued random variable representing either $H^n(\omega)$ for ω fixed in $\mathbb{R}$ or any of the random variables E^n_1, E^n_2, E^n_3, E^n_{13}. The mean value $m_X = \mathscr{E}\{X\}$ is estimated by

$$\widetilde{m}_X = \frac{1}{n_s}\sum_{k=1}^{n_s}X(\theta_k) \tag{33}$$

in which $X(\theta_1),\ldots,X(\theta_{n_s})$ are n_s independent realizations of X. The confidence region associated with this estimate is constructed by using the quantiles. Let F_X be the cumulative distribution function (continuous from the right) of random variable X such that $F_X(x) = P(X \leqslant x)$. For $0 < p < 1$, the pth quantile (or fractile) of F_X is defined by

$$\zeta(p) = \inf\{x : F_X(x) \geqslant p\}. \tag{34}$$

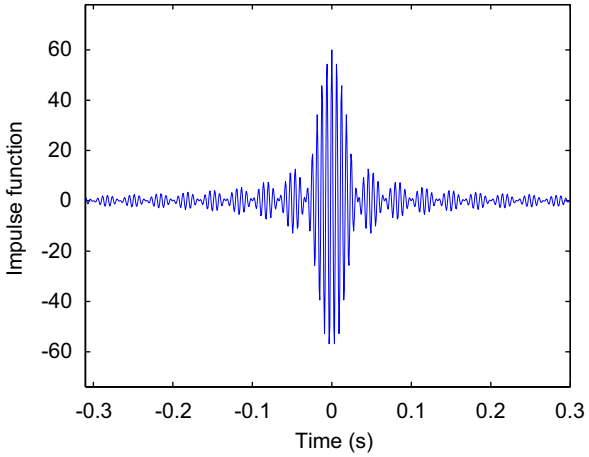

Fig. 1. Impulse function $t \mapsto g(t)$ exciting the system.

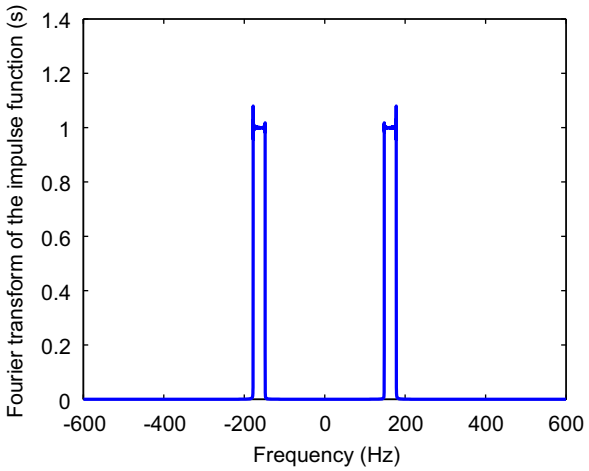

Fig. 2. Fourier transform $f \mapsto \widehat{g}(2\pi f)$ of the impulse function.

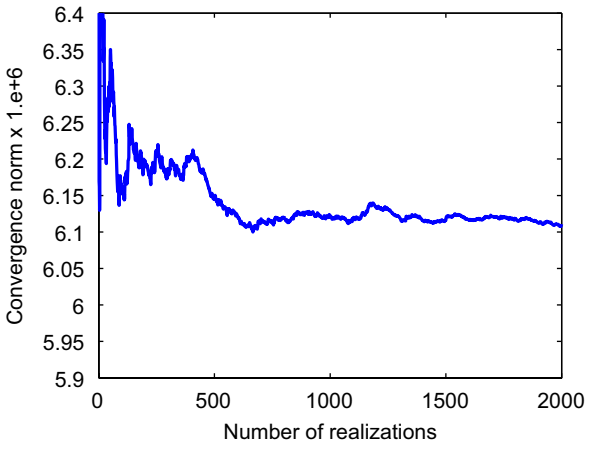

Fig. 3. Mean-square convergence: Function $n_s \mapsto \text{conv}(n_s, n)$ for $n = 40$.

Then the upper envelope x^+ and the lower envelope x^- of the confidence region with probability level P_c are defined by

$$x^+ = \zeta((1+P_c)/2), \quad x^- = \zeta((1-P_c)/2). \tag{35}$$

The estimations of x^+ and x^- are performed by using the sample quantiles. Let $x_1 = X(\theta_1), \ldots, x_{n_s} = X(\theta_{n_s})$. Let $\widetilde{x}_1 < \cdots < \widetilde{x}_{n_s}$ be the order statistics associated with $x_1 < \cdots < x_{n_s}$. The envelopes are then estimated by using

$$x^+ \simeq \widetilde{x}_{j^+}, \quad j^+ = \mathrm{fix}(n_s(1+P_c)/2), \tag{36}$$

$$x^- \simeq \widetilde{x}_{j^-}, \quad j^- = \mathrm{fix}(n_s(1-P_c)/2), \tag{37}$$

where $\mathrm{fix}(z)$ is the integer part of the real number z.

4. Application to a Timoshenko beam with an elastic barrier

This section deals with the application of the theory developed in the previous sections. The linear part of the continuous system is a Timoshenko beam with added dissipation. The nonlinear force is due to a symmetrical linear elastic barrier.

4.1. Description of the nonlinear elastic dynamical system

The geometrical properties of the beam are: length 1 m, width 0.1 m, height 0.1 m. The boundary conditions are of a cantilever beam, with the free end having its motion limited by an elastic barrier at a distance of ε, from both sides of the beam. The gap ε is considered as a parameter. The beam is homogeneous and isotropic, with material properties: density 7500 kg/m^3, Young's modulus 2.1×10^{10} N/m^2, Poisson's coefficient 0.3,

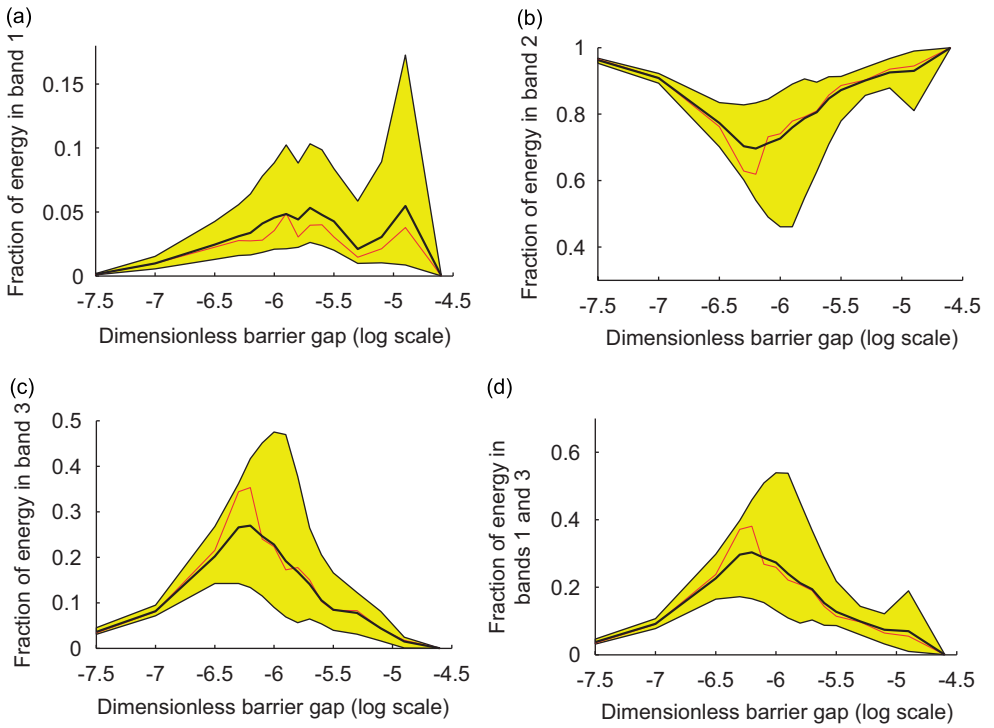

Fig. 4. $\delta_m = 0.1$ and $\delta_b = 0.05$: random fraction functions $\eta \mapsto E_1^n(\eta), E_2^n(\eta), E_3^n(\eta)$ and $E_{13}^n(\eta)$ related to the random mechanical energy transferred to band: (a) B_1; (b) B_2; (c) B_3 and $B_1 \cup B_3$. Mean system (thin solid line). Mean value for the stochastic system (thick solid line). Confidence region (grey region).

shearing correction factor 5/6. The damping model is introduced by seeting the model damping rate to 0.02 for the first three modes, to 0.01 for the fourth mode and to 0.005 for the others. The elasticity constant of the barrier is $\underline{k}_b = 10^7\,\mathrm{N/m}$. The function $\mathbf{f}_{\mathrm{NL}}$ defined in Eq. (1) is then independent of the velocity and is written as

$$f_{\mathrm{NL}}(y) = \begin{cases} 0, & |y| \leqslant \varepsilon, \\ -\underline{k}_b(y - \varepsilon\,\mathrm{sign}(y)), & |y| > \varepsilon. \end{cases} \tag{38}$$

4.2. Mean model

4.2.1. Mean finite element model

The mean finite element model of the cantilever beam consists of 100 2-nodes Timoshenko beam elements. The first six computed eigenfrequencies are 26.9, 162.7, 432.9, 794.1, 1219.2 and 1685.3 Hz.

4.2.2. Description of excitation force

The vector load is defined by Eq. (2). The amplitude a is considered as a parameter. The force is a point force applied at the middle point of the beam. The impulse function g is such that

$$g(t) = \frac{1}{\pi t}\{\sin(t(\Omega_c + \Delta\Omega/2)) - \sin(t(\Omega_c - \Delta\Omega/2))\}, \tag{39}$$

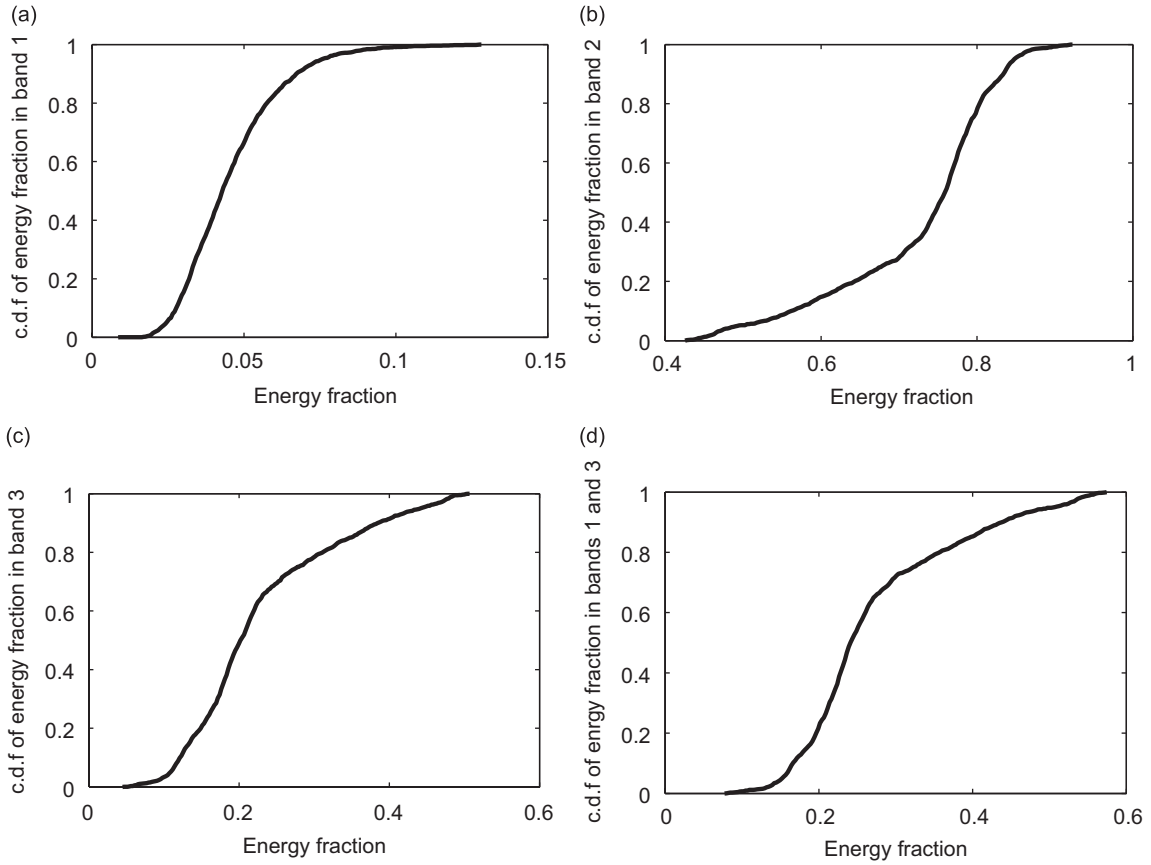

Fig. 5. $\delta_{\mathrm{m}} = 0.1$ and $\delta_b = 0.05$. For $\log_{10}\eta = -6.0$, cumulative distribution function: (a) $\zeta^1 \mapsto \mathrm{Proba}\{E_1^n(\eta) \leqslant \zeta^1\}$; (b) $\zeta^2 \mapsto \mathrm{Proba}\{E_2^n(\eta) \leqslant \zeta^2\}$; (c) $\zeta^3 \mapsto \mathrm{Proba}\{E_3^n(\eta) \leqslant \zeta^3\}$; and (d) $\zeta^{13} \mapsto \mathrm{Proba}\{E_{13}^n(\eta) \leqslant \zeta^{13}\}$ related to the random mechanical energy transferred to band B_1, B_2, B_3 and $B_1 \cup B_3$, respectively.

whose Fourier transform is $\widehat{g}(\omega) = \mathbf{1}_{\underline{B}_2 \cup B_2}$. The frequency band B_2 is defined by Eq. (3) with $\omega_{\min} = 2\pi f_{\min}$ and $\omega_{\max} = 2\pi f_{\max}$ with $f_{\min} = 148\,\text{Hz}$ and $f_{\max} = 178\,\text{Hz}$. The corresponding bandwidth $\Delta\Omega = 2\pi\Delta f$ is then such that $\Delta f = 30\,\text{Hz}$ and the central frequency $\Omega_c = 2\pi f_c$ is such that $f_c = 163\,\text{Hz}$. Consequently, the frequency band of excitation is centered on the second eigenfrequency of the linear system.

4.2.3. Reduced mean model

The numerical results presented in this section are computed with $n = 40$, and the modes were calculated with the finite element model. This value was chosen to assure good convergence for the deterministic and the stochastic solutions.

4.3. Probabilistic model of uncertainties

4.3.1. Parametric probabilistic model of the barrier

Since the gap is taken as a parameter in the problem it is not considered as uncertain. On the other hand, the stiffness in the barrier is uncertain and modelled by a positive-valued random variable K_b whose mean value is $\underline{k}_b$, for which the coefficient of variation δ_b is 0 (no uncertainty) or 0.05 (uncertainty) and whose probability distribution is the Gamma law.

4.3.2. Non-parametric probabilistic model of the beam

As explained in Section 3.3.2, the uncertainty levels for the mass, damping, and stiffness of the linear system are controlled by the dispersion parameters δ_M, δ_D, and δ_K, respectively. In order to simplify the presentation, have only the cases $\delta_M = \delta_D = \delta_K$ are considered. The common valued will be denoted by δ_{m}. Two values are considered $\delta_{\text{m}} = 0$ (no uncertainty) and $\delta_{\text{m}} = 0.1$ (uncertainty).

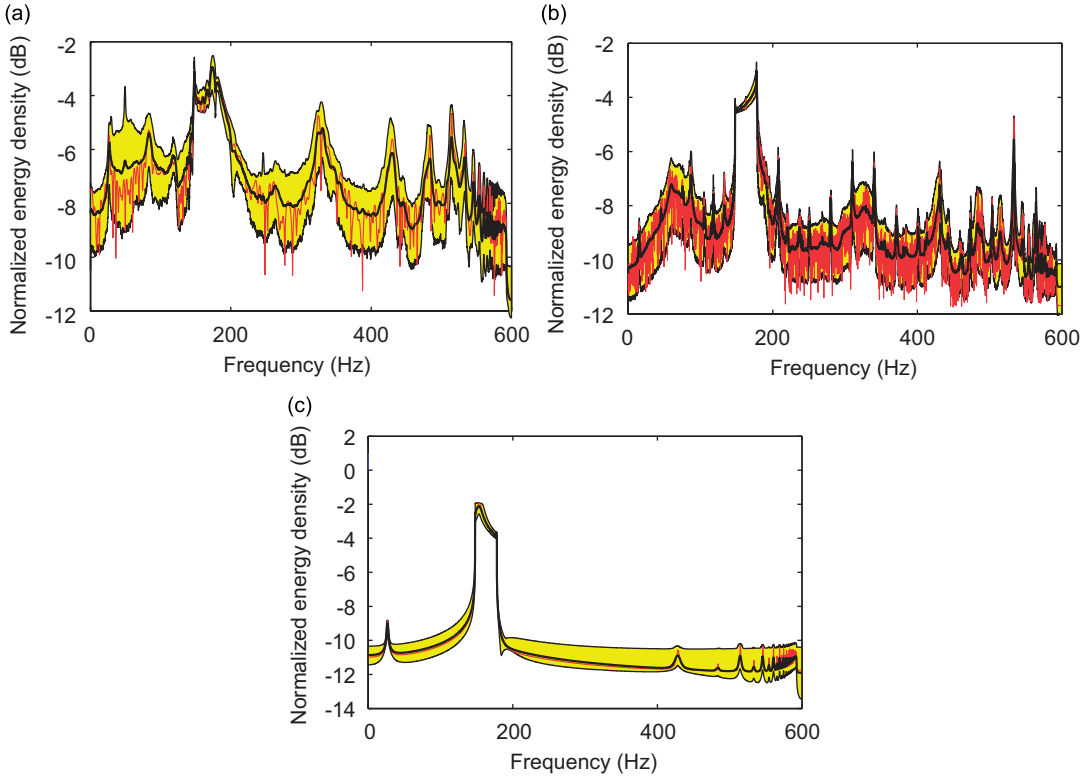

Fig. 6. $\delta_{\text{m}} = 0.1$ and $\delta_b = 0.05$. For (a) $\log_{10}\eta = -6.0$ (b) $\log_{10}\eta = -7.5$ and (c) $\log_{10}\eta = -4.6$, graphs of the random normalized energy density $f \mapsto H^n_{\text{dB}}(2\pi f)$. Mean system (thin solid line). Mean value for the stochastic system (thick solid line). Confidence region (grey region).

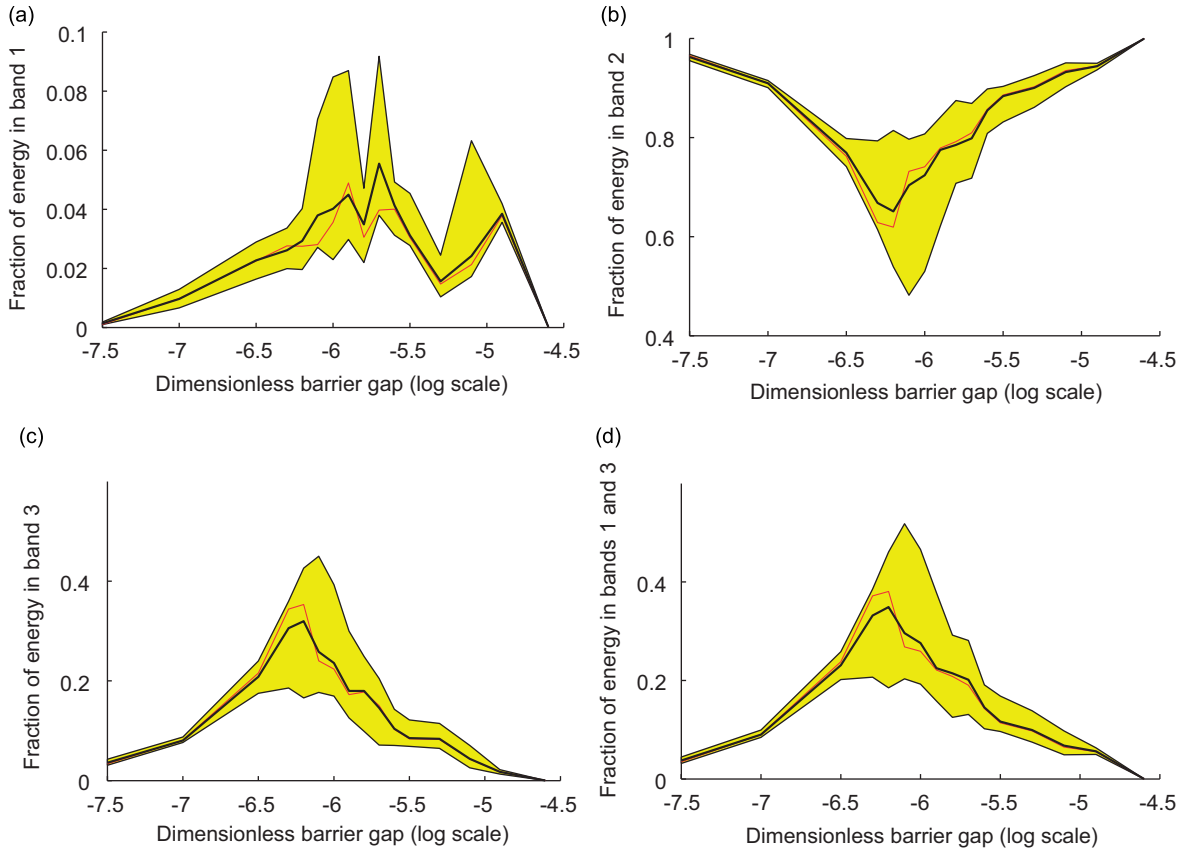

Fig. 7. $\delta_{\mathrm{m}} = 0$ and $\delta_b = 0.05$: Random fraction functions $\eta \mapsto E_1^n(\eta), E_2^n(\eta), E_3^n(\eta)$ and $E_{13}^n(\eta)$ related to the random mechanical energy transferred to band: (a) B_1 (b) B_2; (c) B_3; and (d) $B_1 \cup B_3$. Mean system (thin solid line). Mean value for the stochastic system (thick solid line). Confidence region (grey region).

4.4. Numerical integration parameters

Let $f_0 > f_{\max}$ be the upper frequency such that the total energy of the response of the nonlinear dynamical system is included in the frequency band $[-f_0, f_0]$. For all the numerical results presented below, a convergence analysis has been performed with respect to the value of f_0. The smallest value of f_0 for which all the results converged is $f_0 = 600\,\mathrm{Hz}$ and all the results presented below correspond to this value of f_0. The integration time step is taken as $\Delta t = 1/(2f_0)$ and the time integration $T = n_{\mathrm{time}}\Delta t$ with $n_{\mathrm{time}} = 8192$. The integration in $\mathbb{R}$ is approximated by an integration over the interval $[t_0, t_1]$ in which $t_0 = -T/2$ and $t_1 = T/2 - \Delta t$. The sampling time points are $t_k = t_0 + k\Delta t, k = 0, \ldots, n_{\mathrm{time}} - 1$. Because the Fourier transform is computed by using the FFT algorithm, the integration step in the frequency domain is $\Delta\omega = 2\omega_0/n_{\mathrm{freq}}$ with $n_{\mathrm{freq}} = n_{\mathrm{time}}$. The sampling frequency points are $\omega_k = -\omega_0 + k\Delta\omega, k = 0, \ldots, n_{\mathrm{freq}} - 1$. Eq. (31) is integrated over $[t_0, t_1]$ with zero initial conditions at t_0. The given choice of the parameters are such that $\mathscr{E}\{\|\mathbf{Q}(t_1, \theta)\|^2\}$ is negligible at the final time t_1.

4.5. Numerical results

Fig. 1 is a graph of the impulse function $t \mapsto g(t)$, whose Fourier transform $f \mapsto \widehat{g}(2\pi f)$ is shown in Fig. 2. Fig. 3 is the function $n_s \mapsto \mathrm{conv}(n_s, n)$ defined by Eq. (32) for $n = 40$. The convergence is reached for $n_s \geqslant 1500$. Below, the results are computed with $n_s = 2000$. Recall that $\eta = \varepsilon/a$ is the parameter that is used in the

analysis of the random transferred energies outside the excitation band B_2. All the confidence regions shown in this work correspond to a probability level $P_c = 0.96$.

The other results can be presented in several ways. To save space we show only one of the possible ways as an example. In the next section other forms to analyze the results are suggested. The example we have chosen to present is where the results are arranged by the values of the model and data uncertainties, (δ_m, δ_b). This will give three blocks of results indexed by $(0.1, 0.05)$, $(0, 0.05)$, and $(0.1, 0)$. We present now the first block, the other two are similar. In Fig. 4 are shown the random functions given in Eq. (25) that describe the random function energies in the frequency bands B_1, B_2, B_3, $B_1 \cup B_3$ (Figs. 4(a)–(d), respectively). The mean system results are shown along with the mean of the stochastic system and the associated confidence limits. Fig. 5 shows, for a fixed value of η given by $\log_{10}(\eta) = -6.0$, the cumulative distribution functions of the energies. Fig. 6 shows the density function defined by Eqs. (22) and (23) for three fixed values of η such that $\log_{10}(\eta) = -6.0, -7.5, -4.6$, respectively (Figs. 6(a)–(c), respectively). Similar results (without cumulative distribution functions), for the case $(0, 0.05)$ are shown in Figs. 7 and 8, and for the case $(0.1, 0)$ are shown in Figs. 9 and 10.

5. Analysis of the results and conclusions

5.1. Some remarks about the deterministic narrow-band excitation

As explained in the introduction section, the excitation has been modelled by a deterministic narrow-band signal (see Figs. 1 and 2). Recall that the objective of the paper is to analyze the nonlinear dynamical response of systems excited at a given resonance by a harmonic excitation. Since the mechanical system is uncertain,

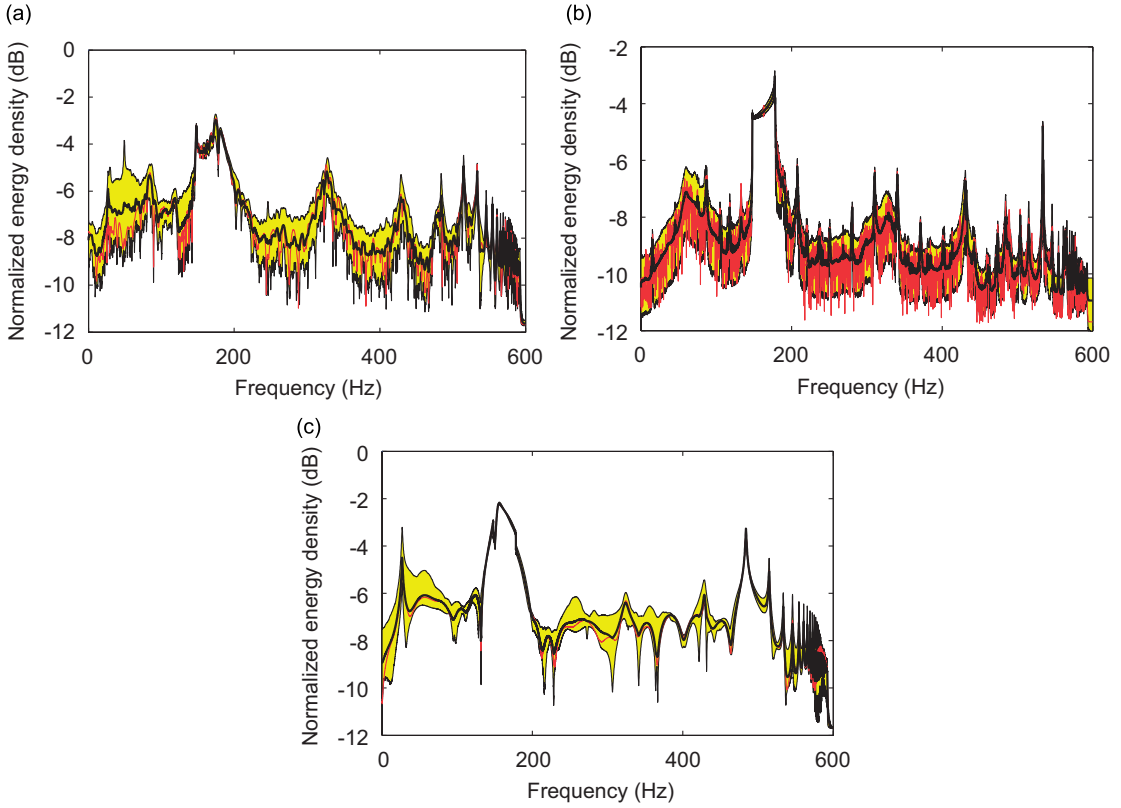

Fig. 8. $\delta_m = 0$ and $\delta_b = 0.05$. For (a) $\log_{10}\eta = -6.0$, (b) $\log_{10}\eta = -7.5$ and (c) $\log_{10}\eta = -4.6$, graphs of the random normalized energy density $f \mapsto H^n_{dB}(2\pi f)$. Mean system (thin solid line). Mean value for the stochastic system (thick solid line). Confidence region (grey region).

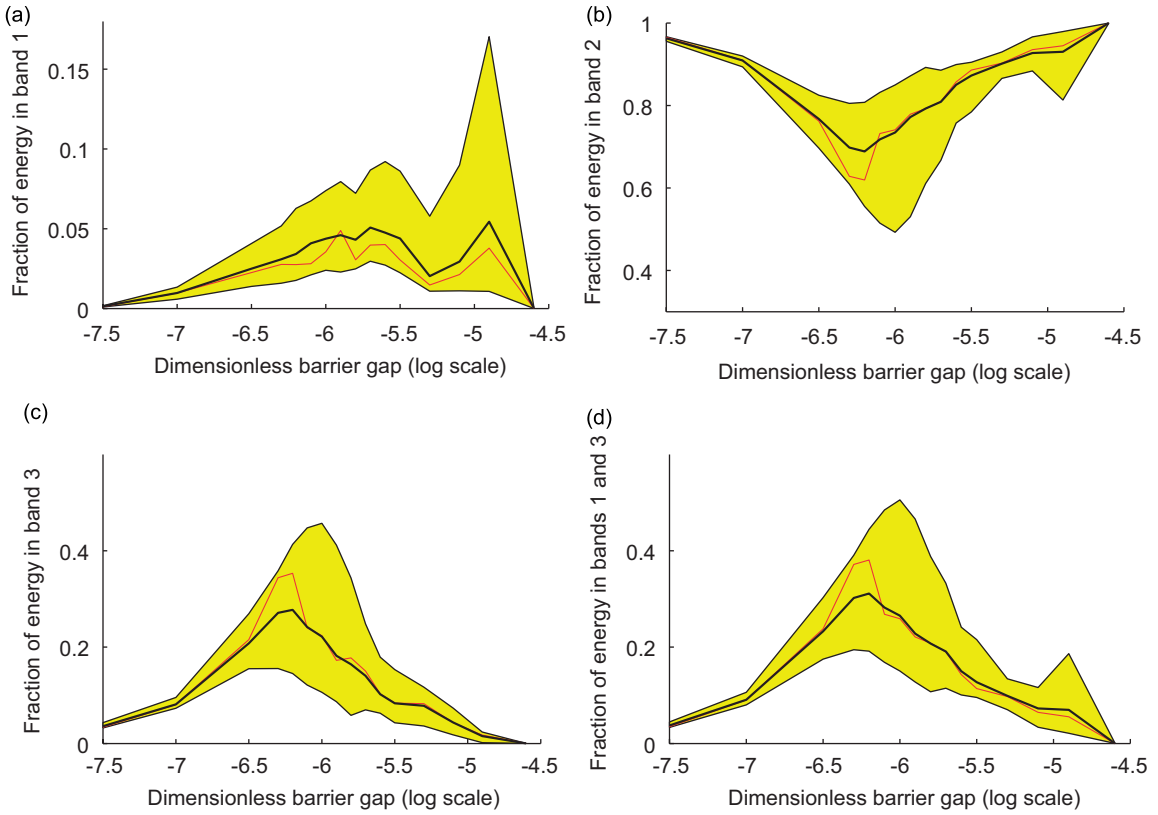

Fig. 9. $\delta_m = 0.1$ and $\delta_b = 0$: random fraction functions $\eta \mapsto E_1^n(\eta), E_2^n(\eta), E_3^n(\eta)$ and $E_{13}^n(\eta)$ related to the random mechanical energy transferred to band: (a) B_1, (b) B_2, (c) B_3 and (d) $B_1 \cup B_3$. Mean system (thin solid line). Mean value for the stochastic system (thick solid line). Confidence region (grey region).

a narrow-band signal is chosen in order to give robustness to this excitation. Fig. 6 shows that the considered resonance of the uncertain system is effectively excited by the chosen narrow-band signal.

5.2. Maximum of nonlinearity effects as a function of η

The measures of nonlinearity is given by the fraction of energy that is transferred outside the band of excitation. Figs. 4, 7 and 9 show that a maximum of nonlinearity effect is obtained for mid-value of $\eta = \varepsilon/a$ and not for the extremes, near zero or very large. Near zero means that the gap is very small with respect to the displacement, that is there are a large number of impacts with low energy (small gap). This case is frequent, for instance, in Robotics (looseness). Very large means that the gap is sufficiently big with respect to the displacement such that the number of impacts is small and with low energy. In the medium range, the impacts are more frequent and also more energetic. It is worthwhile to note that as η is the ratio of the gap and the amplitude of the excitation, even for very small gaps the effect of η can be large depending on the force. For example, for $\varepsilon = 2 \times 10^{-6}$ m, a force of 1 N corresponds to a numerical value of $\eta = 2 \times 10^{-6}$, and Fig. 4(d) shows that for this value there is a transfer of 30–50 percent of the energy outside the band of excitation.

5.3. Relation of the nonlinearities with the spectral density

Figs. 6(b), 8(b) and 10(b) (corresponding to $\eta = 10^{-7.5}$, a near zero gap case) shows that although there is a small amount of energy transferred outside the band of excitation the effect of this transfer on the spectral density is very large causing the response to become a broad-band signal. From Figs. 6(c), 8(c) and (10c)

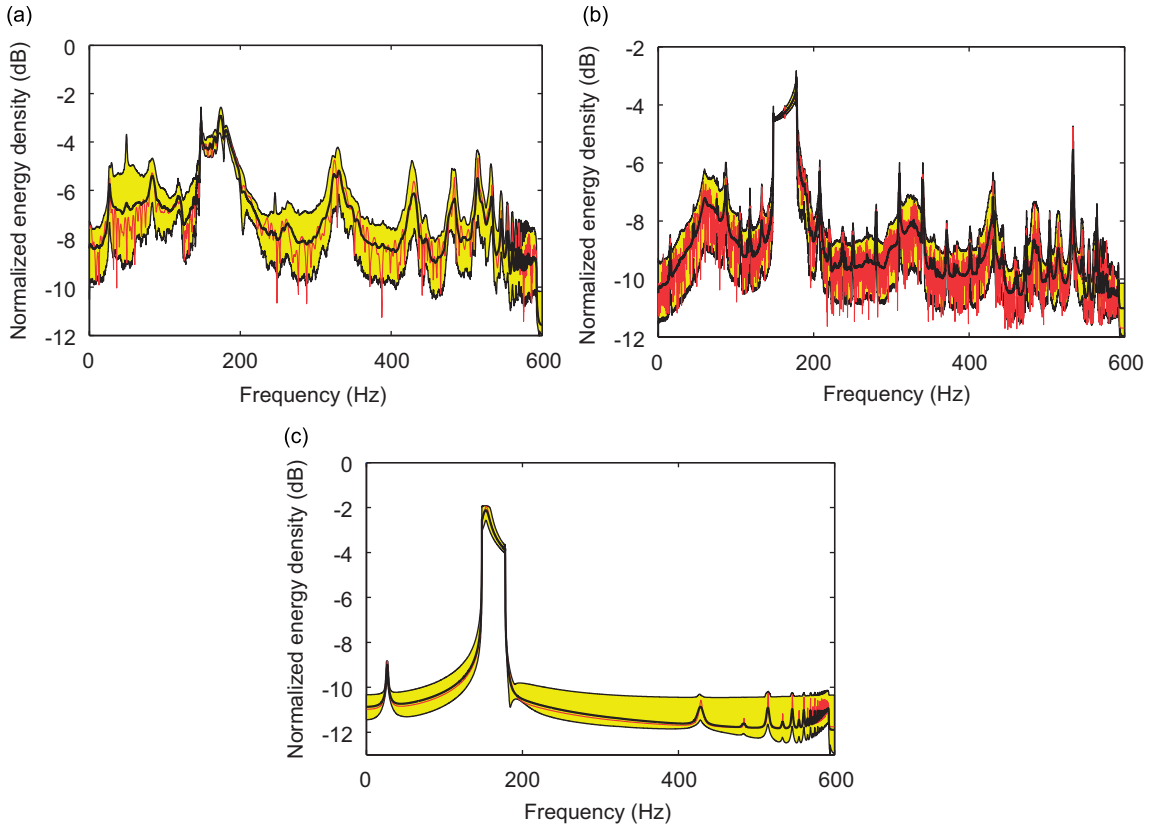

Fig. 10. $\delta_m = 0.1$ and $\delta_b = 0$. For (a) $\log_{10}\eta = -6.0$, (b) $\log_{10}\eta = -7.5$ and (c) $\log_{10}\eta = -4.6$, graphs of the random normalized energy density $f \mapsto H^n_{dB}(2\pi f)$. Mean system (thin solid line). Mean value for the stochastic system (thick solid line). Confidence region (grey region).

($\eta = 10^{-4.6}$, which is a very large gap case) it can be seen that there is a very small amount of energy transferred outside the band of excitation so the system is nearly linear.

5.4. Uncertainties effects

It can be seen in Fig. 4 that the point of maximum energy transfer due to nonlinearities is also the point of less robustness with respect to uncertainties. On the other hand, the two limiting cases, near zero and very large η, are relatively robust with respect to uncertainties. The effect of two types of uncertainties: barrier uncertainties and model uncertainties for the continuous linear system are now discussed. Fig. 7 (corresponding to barrier uncertainties) and Fig. 9 (corresponding to model uncertainties) clearly show that the nonlinearity effects are less robust for model uncertainties than for barrier uncertainties. This statement results from the following considerations. There is a loss of robustness induced by barrier uncertainties and by model uncertainties in the continuous linear subsystems (see Figs. 7(d) and 9(d)) where the confidence region are significantly large. Comparing Fig. 4(d) with Fig. 9(d) shows that the two confidence regions are almost equal. This means that the effect of barrier uncertainties are less than the effects of model uncertainties. In addition, it can be seen that the confidence region in Fig. 7(d) is included (set inclusion) in the confidence region of Fig. 4(d). Also from Figs. 6(a), 8(a) and 10(a) it can be seen that the maximum nonlinearity effects on the frequency response in the sub-harmonic and super-harmonic ranges is less robust for model uncertainties than for barrier uncertainties. On the other hand, the frequency response in the frequency band of excitation is robust with respect to uncertainties. The probability of the random energies can be estimated from the data in

Fig. 5. For instance, from Fig. 5(d) it can be seen that the probability for greater than 20% of the energy to be transferred outside the band of excitation is 0.75, and to be larger than 40 percent the probability is 0.20.

5.5. Scope of the proposed method and its limitations

It should be noted that the external excitation force is a narrow-band signal that is completely known. In this context, the proposed method can be used to me as we the nonlinearity effects for the entire system. However, with this method it is not possible to measure the nonlinearity effects of its subsystems.

The probabilistic approach presented can be used on any system composed of a continuous linear subsystem (for instance, a Timoshenko beam) coupled with any discrete nonlinear subsystem (for instance, an elastic barrier). Nevertheless, this kind of approach cannot be applied to a nonlinear continuous system such as an elastic system with large deformations. For such a case additional developments are required.

Acknowledgments

This work was supported by the Brazilian Agency Conselho Nacional de Desenvolvimento Científico e Tecnológico (CNPq), by the International Cooperation Project Capes-Cofecub, No. 476/04, and Faperj.

References

[1] V.I. Babitsky, N. Birkett, *Theory of Vibro-impact Systems and Applications*, Springer, Berlin, 1998.
[2] M.F. Dimentberg, A.A. Sokolov, Identification of restoring force nonlinearity from system's response to a white-noise excitation, *International Journal of Non-Linear Mechanics* 26 (6) (1991) 851–855.
[3] M.F. Dimentberg, D.V. Iourtchenko, Random vibrations with impacts: a review, *Nonlinear Dynamics* 36 (2004) 229–254.
[4] J.P. Cusumano, M.T. Sharkady, B.W. Kimble, Dynamics of a flexible beam impact oscillator, *Philosophical Transactions of the Royal Society of London* 347 (1994) 421–438.
[5] R. Bouc, M. Defilippi, Multimodal nonlinear spectral response of a beam with impact under random input, *Probabilistic Engineerings Mechanics* 12 (3) (1997) 163–170.
[6] E. Emaci, T.A. Nayfeh, A.F. Vakakis, Numerical and experimental study of nonlinear localization in a flexible structure with vibro-impacts, *Zeitschrift für Angewandte Mathematik und Mechanik (ZAMM)* 77 (1997) 527–541.
[7] C. Wolter, M.A. Trindade, R. Sampaio, Reduced-order model for an impacting beam using the Karhunen-Loève expansion, *Tendências em Matematica Aplicada e Computacional, TEMA* 3 (2) (2002) 217–226.
[8] M.A. Trindade, C. Wolter, R. Sampaio, Karhunen-Loève decomposition of coupled axial-bending vibrations of beams subject to impacts, *Journal of Sound and Vibration* 279 (3–5) (2005) 1015–1036.
[9] C. Soize, A nonparametric model of random uncertainties for reduced matrix model in structural dynamics, *Probabilistic Engineering Mechanics* 15 (3) (2000) 277–294.
[10] C. Soize, Random matrix theory for modeling uncertainties in computational mechanics, *Computer Methods in Applied Mechanics and Engineering* 194 (12–16) (2005) 1333–1366.
[11] C.E. Shannon, A mathematical theory of communications, *Bell System Technical Journal* 27 (1948) 379–423.
[12] E.T. Jaynes, Information theory and statistical mechanics, *Physical Review* 106 (4) (1957) 620–630.
[13] E.T. Jaynes, Information theory and statistical mechanics, *Physical Review* 108 (2) (1957) 171–190.